Excitability of prefrontal cortical pyramidal neurons is modulated by activation of intracellular type-2 cannabinoid receptors

Femke S. den Boon[a,1], Pascal Chameau[a,1], Qiluan Schaafsma-Zhao[a], Willem van Aken[a], Monica Bari[b,c], Sergio Oddi[c,d], Chris G. Kruse[a], Mauro Maccarrone[c,d,2], Wytse J. Wadman[a,2], and Taco R. Werkman[a,2,3]

[a]Center for Neuroscience, Swammerdam Institute for Life Sciences, University of Amsterdam, 1098 XH, Amsterdam, The Netherlands; [b]Department of Experimental Medicine and Biochemical Sciences, Tor Vergata University, 00133 Rome, Italy; [c]European Center for Brain Research/Santa Lucia Foundation, 00179 Rome, Italy; and [d]Department of Biomedical Sciences, University of Teramo, 64100 Teramo, Italy

Edited by Leslie Lars Iversen, University of Oxford, Oxford, United Kingdom, and approved January 20, 2012 (received for review November 4, 2011)

The endocannabinoid (eCB) system is widely expressed throughout the central nervous system (CNS) and the functionality of type-1 cannabinoid receptors in neurons is well documented. In contrast, there is little knowledge about type-2 cannabinoid receptors (CB_2Rs) in the CNS. Here, we show that CB_2Rs are located intracellularly in layer II/III pyramidal cells of the rodent medial prefrontal cortex (mPFC) and that their activation results in IP_3R-dependent opening of Ca^{2+}-activated Cl^- channels. To investigate the functional role of CB_2R activation, we induced neuronal firing and observed a CB_2R-mediated reduction in firing frequency. The description of this unique CB_2R-mediated signaling pathway, controlling neuronal excitability, broadens our knowledge of the influence of the eCB system on brain function.

calcium-activated chloride current | firing rate | whole-cell current | voltage clamp | intracellular calcium stores

The endocannabinoid (eCB) system is involved in many functions of the CNS, including executive functions associated with the prefrontal cortex, such as decision-making and working memory (1). The eCB system consists of at least two G protein-coupled receptors (GPCRs), type-1 cannabinoid receptor (CB_1R) and type-2 cannabinoid receptor (CB_2R), lipid endogenous ligands (e.g., anandamide and 2-arachidonoylglycerol), and various enzymes responsible for the synthesis and degradation of the endogenous ligands (2–6). CB_1Rs are among the most abundantly expressed GPCRs in the rat brain and their role, predominantly as presynaptic receptors, in modulating neurotransmission is clearly established (5, 7, 8). In contrast with CB_1R, the presence and function of CB_2R in the brain has long been a matter of debate (9). CB_2Rs are found primarily in the immune system and were initially regarded as the "peripheral" cannabinoid receptor (10, 11). This generally accepted idea is challenged by the description of CNS CB_2R gene expression in rats and wild-type mice (12–14) and the identification of functional CB_2Rs on glial cells and neurons (15–18). In addition to the current view that supports the expression of functional CB_2Rs in neurons upon brain stress or damage (19), it has been reported that CB_2Rs could play a role in general CNS physiology (20–22). These developments emphasize the importance of understanding how CB_2R activation affects neuronal functioning. To demonstrate the presence of functional CB_2Rs in the rodent medial prefrontal cortex (mPFC) and to elucidate their functional role, we used Western blotting, a radioactive binding assay, and electrophysiological techniques (whole-cell current and voltage clamp) on layer II/III pyramidal neurons.

Results

Functional CB_2Rs in the mPFC. The presence of CB_2Rs in the rat mPFC was demonstrated by a Western blot performed on homogenated mPFC samples (Fig. 1*A*). A band of the expected molecular weight for CB_2R was detected, which was absent when the primary antibody was incubated with immunizing peptide (Fig. 1*A*). Immunoblots on tissues from spleen and brainstem (positive controls) and skeletal muscle tissue (negative controls) confirmed the specificity of the CB_2R immunodetection (Fig. 1*A*).

To investigate whether CB_2R activation can modulate ion conductances, we performed whole-cell current clamp recordings in layer II/III pyramidal neurons of the mPFC at an experimental membrane potential (Vm = −80 mV) that differed from all experimental ion equilibrium potentials. We observed that bath applications of the selective CB_2R agonist JWH-133 (1 μM and 5 μM) resulted in a transient depolarization in most (86%) layer II/III pyramidal neurons of the mPFC, after a delay that lasted several minutes (Fig. 1 *B* and *C*). The depolarization induced by bath application of 1 μM JWH-133 was significantly smaller after preincubation of the slice with a selective CB_2R antagonist, Sch.356036 (5 μM) (Fig. 1*C*). We confirmed the pharmacological evidence that the depolarization is mediated by CB_2R activation by performing similar experiments in CB_2R knockout (KO) and wild-type (Wt) mice. We did not observe a delayed depolarizing response in mPFC neurons from KO mice, whereas in Wt mice such responses could be evoked (Fig. 1*C*).

To investigate the origin of the depolarization delay, we repeated the experiments but replaced the bath application by fast local pressure ejection of 5 μM JWH-133 onto the soma of patched layer II/III pyramidal neurons. Because the depolarization delay was hardly affected (Fig. 1 *C* and *D*), we concluded that it did not originate from diffusion limitations in the bath application method. We hypothesized that CB_2Rs are located intracellularly in these neurons and that the depolarization delay most likely originates from the time required for the lipophilic ligands to pass the plasma membrane and to reach the intracellularly located target. To test this hypothesis, we introduced 5 μM JWH-133 into the cell via the patch pipette and we still observed a depolarization (Fig. 1*C*), but with a much reduced delay (≈1.5 min) after going whole-cell (Fig. 1*D*). Introduction of the antagonist Sch.356036 (1 μM) into the cell via the patch pipette largely prevented the membrane depolarization induced by bath application of 1 μM JWH-133 (Fig. 1*C*). When the antagonist

Author contributions: F.S.d.B., P.C., M.B., S.O., M.M., and T.R.W. designed research; F.S.d.B., P.C., Q.S.-Z., W.v.A., M.B., and S.O. performed research; C.G.K. contributed new reagents/analytic tools; F.S.d.B., P.C., M.B., S.O., M.M., W.J.W., and T.R.W. analyzed data; F.S.d.B., P.C., M.M., W.J.W., and T.R.W. wrote the paper; W.J.W. supervised the project; and T.R.W. supervised and managed the project.

The authors declare no conflict of interest.

This article is a PNAS Direct Submission.

[1]F.S.d.B. and P.C. contributed equally to this work.

[2]M.M., W.J.W., and T.R.W. contributed equally to this work.

[3]To whom correspondence should be addressed. E-mail: t.r.werkman@uva.nl.

This article contains supporting information online at www.pnas.org/lookup/suppl/doi:10.1073/pnas.1118167109/-/DCSupplemental.

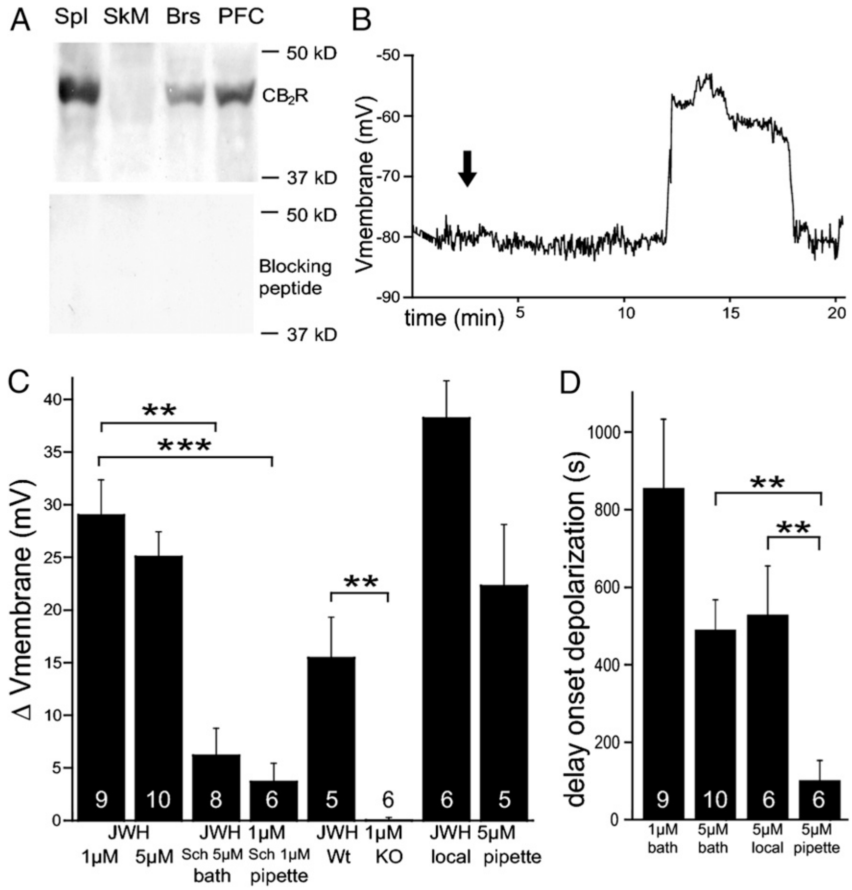

Fig. 1. CB_2Rs are present in the rodent mPFC, and their activation evokes a delayed depolarization. (*A*) Western blot detection of CB_2Rs in the rat mPFC (*Upper*). Primary antibody preincubated with immunogen peptide showed no CB_2R bands (*Lower*). Positive controls: spleen (Spl) and brainstem (Brs); negative control: skeletal muscle (SkM). (*B*) Bath-applied JWH-133 (1 μM, arrow indicates the start of the application) induced a delayed (10 min) depolarization of a layer II/III pyramidal neuron. (*C*) Bath application of 1 and 5 μM JWH-133 induced similar depolarizations ($\Delta V = 29 \pm 3$ mV and 25 ± 2 mV, both $P < 0.001$). After preincubation with 5 μM Sch.356036, application of 1 μM JWH-133 resulted in a significantly reduced depolarization (**$P < 0.01$, Mann–Whitney *U* test). JWH-133 (1 μM) depolarized neurons of Wt mice, but not of CB_2R KO mice ($\Delta V = 15 \pm 4$ mV and 0 ± 0.3 mV; **$P < 0.01$). Local application of JWH-133 (5 μM) with a Picospritzer device and introduction of JWH-133 (5 μM) into neurons via the patch pipette also depolarized neurons ($\Delta V = 38 \pm 4$ mV and 22 ± 6 mV; $P < 0.0001$ and $P < 0.05$). Sch.356036 (1 μM), introduced into neurons via the patch pipette, largely prevented the depolarization by JWH-133 (1 μM, $\Delta V = 4 \pm 2$ mV; ***$P < 0.001$). (*D*) The delays of onset of depolarization after bath application of JWH-133 (1 and 5 μM) and local application of JWH-133 (5 μM) were 855 ± 177 s, 490 ± 76 s, and 529 ± 125 s, respectively. Introduction of JWH-133 (5 μM) via the patch pipette reduced the delay of onset of the effect compared with the other application methods with 5 μM JWH-133 (103 ± 50 s; both **$P < 0.01$, Mann–Whitney *U* tests). Numbers of observations are indicated in bars (*C* and *D*); error bars represent SEM.

Sch.356036 was bath applied, 5 μM was needed to antagonize the JWH-133 (1 μM) effect (Fig. 1*C*). Taken together, the combined electrophysiological and pharmacological experiments suggest an intracellular localization of the CB_2R.

CB_2Rs Are Intracellularly Localized in the mPFC. To obtain further evidence for an intracellular localization for CB_2Rs, we performed additional Western blot experiments. Whole mPFC samples were fractionated into a plasma membrane and an intracellular fraction. The identity of the fractions was established by using antibodies against the plasma membrane marker Na^+/K^+-ATPase and the intracellular marker nucleoporin. The Western blot on fractionated samples showed that CB_2Rs are abundantly present in the intracellular fraction, whereas they are hardly detectable in the plasma membrane fraction (Fig. 2*A*). Experiments using a radioactive binding assay on similarly fractionated mPFC samples corroborated the intracellular localization of CB_2Rs (Fig. 2*B*). Intracellular binding of $[^3H]$CP55.940 (a mixed CB_1R/CB_2R agonist) was reduced by ≈50% in the presence of the selective CB_2R antagonist SR2 (SR144528), but not when the selective CB_1R antagonist SR1 (SR141716) was present. Incubating the plasma membrane fraction with SR1 or SR2 reduced the binding of $[^3H]$CP55.940. However, this reduction in binding was much larger in the presence of SR1 (≈70% reduction) than in the presence of SR2 (≈20% reduction). These results confirm that CB_2R binding sites are predominantly located intracellularly in the rat mPFC, whereas CB_1R binding sites appear to be mainly present in the plasma membrane. In additional fluorescence imaging experiments on a neuronal cell line (human SH-SY5Y neuroblastoma cells transiently transfected with GFP-tagged CB_2Rs), we demonstrated that CB_2Rs are almost exclusively localized in intracellular membranous structures and that they are not present on the plasma membrane (Fig. S1 and Table S1).

CB_2R Activation Opens Ca^{2+}-Activated Cl^- Channels via IP_3R. The signaling cascade after CB_2R activation can lead, through phospholipase C production, to Ca^{2+} release via IP_3R (23) and, thus, to the potential activation of Ca^{2+}-activated conductances (24). Introduction of the fast Ca^{2+} chelator 1,2-bis(2-aminophenoxy) ethane-*N,N,N′,N′*-tetraacetic acid (BAPTA) at a high concentration (10 mM) into the cell via the patch pipette, strongly reduced

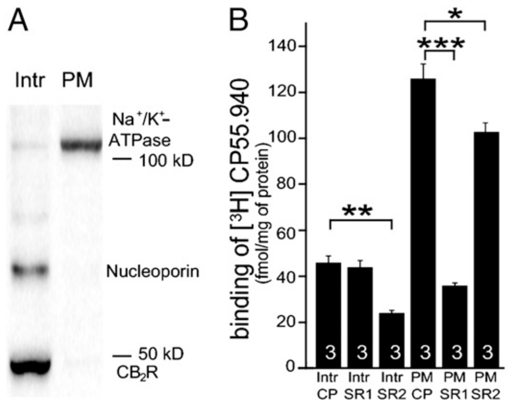

Fig. 2. CB_2Rs are localized intracellularly in the rat mPFC. (*A*) Western blot on subcellular mPFC fractions, consisting of an intracellular fraction (Intr) and a plasma membrane fraction (PM), demonstrated a predominantly intracellular localization of CB_2R. Membranes were probed with antibodies against CB_2R, the intracellular marker nucleoporin, and the plasma membrane marker Na^+/K^+-ATPase. (*B*) Radioactive binding experiments show that intracellular binding of the mixed CB_1R/CB_2R agonist [^{3}H]CP55.940 (CP; 46 ± 3 fmol/mg) was reduced in the presence of SR2 (a CB_2R antagonist; 24 ± 1 fmol/mg; $^{**}P < 0.01$) and not in the presence of SR1 (a CB_1R antagonist; 44 ± 3 fmol/mg). Plasma membrane binding of [^{3}H]CP55.940 (126 ± 6 fmol/mg) was reduced after incubation with SR1 (36 ± 1 fmol/mg; $^{***}P < 0.001$) or SR2 (102 ± 4 fmol/mg; $^{*}P < 0.05$). The reduction of plasma membrane binding was significantly larger in the presence of SR1 compared with SR2 (71 ± 1% and 19 ± 4%, respectively; $P < 0.001$). Numbers of observations are indicated in bars; error bars represent SEM.

the amplitude of the delayed depolarization (Fig. 3*A*). Bath application of the IP_3R blocker 2-aminoethyl diphenylborinate (2-APB, 0.1 mM) also reduced the depolarization evoked by JWH-133 (Fig. 3*A*). These results indicate that a rise in $[Ca^{2+}]_i$ after IP_3R activation is necessary for the CB_2R-mediated depolarization. A series of voltage clamp experiments was performed to determine which conductance underlies the CB_2R-mediated depolarization. Application of JWH-133 (1 μM) decreased the input resistance (R_{input}; Fig. 3*B*), implying that the signal transduction pathway after CB_2R activation opens ion channels in the plasma membrane. Using a series of step potentials before and during the JWH-133 application allowed the construction of a current-voltage (I/V) relationship that reversed near the calculated reversal potential (E_{rev}) for Cl^- (E_{Cl-}) (Fig. 3*C*). Blocking K^+, Ca^{2+}, and Na^+ channels with 4-aminopyridine (4-AP), tetraethylammonium-Cl (TEACl), Cd^{2+}, and tetrodotoxin (TTX) hardly had an effect on the magnitude and the reversal potential of the currents evoked by JWH-133 (Fig. 3*D*). In addition, decreasing $[Cl^-]_i$ to 4.95 mM shifted E_{rev} toward the newly established E_{Cl-} (Fig. 3*D*). We observed similar currents when we used a different selective CB_2R agonist, HU-308 (1 μM) (Fig. 3*D, Inset*). Finally, the JWH-133–evoked currents were markedly reduced in the presence of the Cl^- channel blocker 4,4′-diisothiocyanatostilbene-2,2′-disulfonic acid (DIDS) (Fig. 3*E*). In summary, these results show that CB_2R activation leads to the opening of Ca^{2+}-activated Cl^- channels (CaCCs) that may contribute to the control of the membrane potential of layer II/III pyramidal neurons of the rat mPFC.

CB_2R Activation Reduces Neuronal Excitability. The hypothesis that the CB_2R-mediated signaling pathway contributes to neuronal excitability was further investigated in a series of current clamp experiments under physiological Cl^- conditions (E_{Cl-} = −70 mV). A "slow" automatic feedback system ensured that recordings always started at a membrane potential of −70 mV. Neuronal firing was evoked by Gaussian current input into the soma, via the patch pipette, that evoked fluctuations around resting membrane potential. For each neuron, the variance of the input signal was adjusted to cause a stable spiking rate (≈0.85 Hz). Application of 1 μM JWH-133 reduced the firing rate by 45%, and this reduction could be prevented by preincubation (of at least 10 min) with the CB_2R antagonist, Sch.356036 (5 μM) (Fig. 4). In a separate experiment, we tested the effect of Sch.356036 by itself on the firing rate. Application of 5 μM Sch.356036 increased the firing rate (mean baseline firing frequency of 0.86 ± 0.09 Hz was normalized over slices to 100 ± 8% and increased to 121 ± 8% in the presence of Sch.356036, $P < 0.05$, $n = 12$). These results indicate an endogenous tonus of eCBs and/or constitutive activity of the receptor and show that, when firing is evoked with an input that could resemble spontaneous background synaptic activity, further CB_2R activation modulates the firing rate of mPFC neurons.

Discussion

Our results provide evidence for functional neuronal CB_2Rs that are located intracellularly, in the rodent mPFC. Their activation results, via IP_3R activation, in the opening of CaCCs. Furthermore, this opening of CaCCs is most likely responsible for the observed reduction in neuronal excitability upon CB_2R activation. The presence of CB_2R mRNA in the brain and CB_2Rs in neurons of the brainstem, the cerebellum, and the hippocampus has been reported (12, 13, 18, 25–28), but their presence in the cortex remained to be further characterized. The current view on the presence of functional CB_2Rs in the CNS supports the expression of CB_2Rs in neurons essentially upon brain stress and damage (19). Commonplace problems with the visualization of CB_2Rs by immunohistochemical stainings have been described. These problems may arise from the difficulty of producing reliable antibodies against CB_2Rs, slight differences in diaminobenzidine (DAB) staining protocols, species-specific isoform expression patterns and complications with negative controls such as CB_2R-KO (9, 14, 28, 29). Therefore, we used a combination of biochemical (Western blotting and radioactive binding assay) and functional (in vitro electrophysiology and pharmacology) techniques to provide evidence that functional CB_2Rs are expressed intracellularly in cortical neurons of the healthy brain. The results of the radioactive binding assay did not depend on the quality of antibodies and provided additional support for the intracellular presence of CB_2Rs in the mPFC where this technique confirmed that CB_1Rs are primarily located in the plasma membrane. In addition, by means of fluorescence imaging, we could demonstrate that in a neuronal cell line (human neuroblastoma cells; *SI Materials and Methods*) CB_2Rs are predominantly located in intracellular membranous structures and not in the plasma membrane. In accordance with our results, a few publications support the idea that, like other functional GPCRs (30, 31), functional CB_2Rs may have an intracellular localization. A report by Currie et al. (32) shows the intracellular localization of functional CB_2Rs in guinea pig heart cells. Others report that CB_2Rs are associated with the rough endoplasmic reticulum and Golgi apparatus in hippocampal pyramidal neurons, but in these studies, the functional role of intracellular CB_2Rs was not investigated (25, 26, 28).

The CB_2R signaling pathway shows great diversity and complexity (33) and has not been fully elucidated in neurons. The main downstream signaling pathway of CB_2R activation involves Gi/o and the subsequent modulation of adenylate cyclase and MAP kinase activity (34), but coupling to the modulation of $[Ca^{2+}]_i$ has also been reported (33). In calf pulmonary endothelial cells, activation of CB_2Rs by anandamide resulted in an increase in $[Ca^{2+}]_i$, mediated by PLC activation and IP_3 production (23). In cardiac cells (32) and adult dorsal root ganglion neurons (35), CB_2R activation was reported to be negatively coupled to IP_3R-mediated Ca^{2+} release. In addition to the known CB_2R-mediated pathways, we demonstrate that in rodent layer II/III cortical

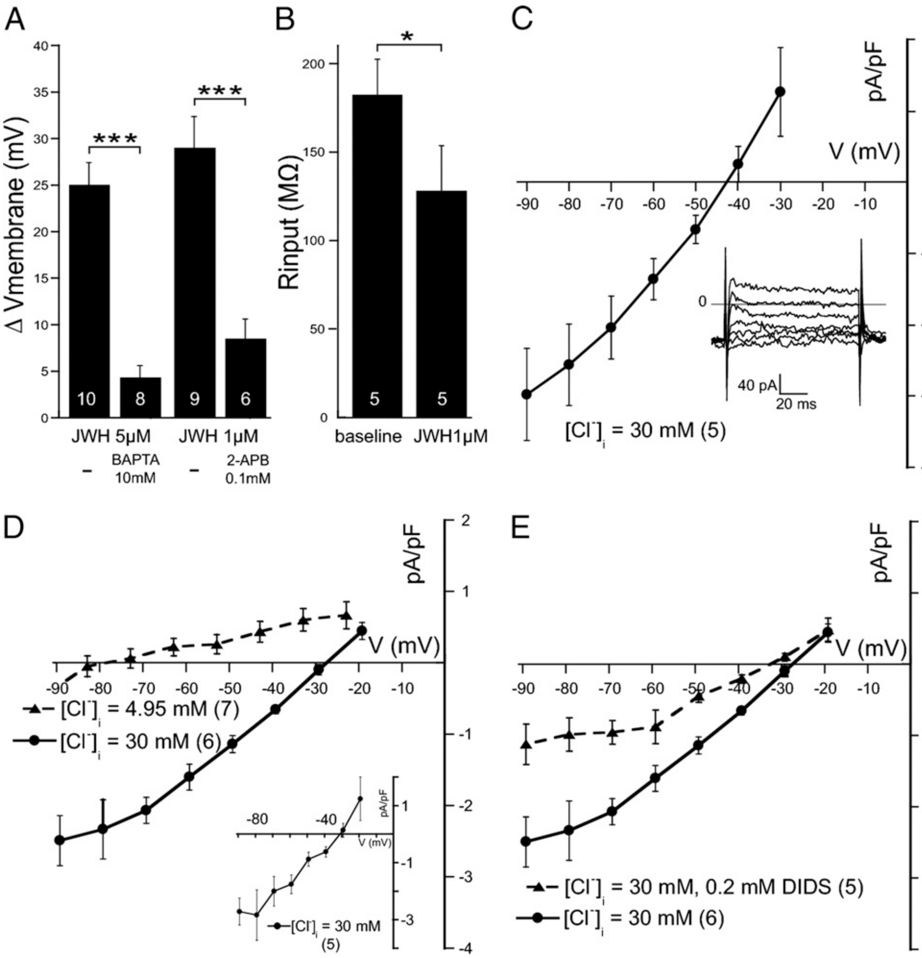

Fig. 3. CB_2R activation evokes an IP_3R-dependent opening of Ca^{2+}-activated Cl^- channels. (*A*) In the presence of either 10 mM BAPTA in the patch pipette or 0.1 mM 2-APB in the bath, 5 μM or 1 μM JWH-133 evoked significantly reduced (both $^{***}P < 0.001$) depolarizations ($\Delta V = 4 \pm 1$ mV and 8 ± 2 mV). The average response evoked with 5 μM JWH-133 (in the absence of BAPTA) is the same as is depicted in Fig. 1*C*. (*B*) The input resistance (R_{input}) was reduced by JWH-133 (182 ± 20 MΩ and 128 ± 25 MΩ; $^{*}P < 0.05$). (*C*) I/V relationship of CB_2R-mediated currents (evoked with 1 μM JWH-133) that reverse at -40 ± 2mV, close to E_{Cl-} (−38.3 mV); *Inset* shows representative current traces. (*D*) In the presence of 4-AP, TEACl, Cd^{2+}, and TTX (to block K^+, Ca^{2+}, and Na^+ channels) and recorded with $[Cl^-]_i = 30$ or 4.95 mM, E_{rev} of CB_2R-mediated currents (-26 ± 2 mV and -76 ± 4 mV) followed E_{Cl-} (−32.6 mV and -80 mV). (*D Inset*) Another selective CB_2R agonist, HU-308 (1 μM), evoked similar currents (E_{rev}: -31 ± 2 mV, E_{Cl-}: −32.6 mV). (*E*) The Cl^- channel blocker DIDS (0.2 mM) reduced the amplitude of CB_2R-mediated currents. Numbers of observations are indicated in bars/brackets; error bars represent SEM.

pyramidal neurons, the CB_2R signaling cascade involves IP_3R activation and results in the opening of CaCCs. CaCCs are known to control excitability in various types of peripheral and central neurons (24, 36), but have not been described in pyramidal neurons of the mPFC.

Although some publications report a functional role for CB_2Rs in the CNS (20–22), the precise mode of action is not known. In this study, we demonstrate that CB_2R activation—under physiological conditions—leads to a decrease in neuronal firing rate, probably via the opening of CaCCs. If E_{Cl-} is close to the resting membrane potential of cortical neurons, the activation of CB_2Rs will stabilize or even clamp the membrane potential around that level. This reduction of neuronal excitability upon CB_2R activation is reminiscent of shunting inhibition, described for $GABA_A$ receptors (37, 38), that also mediate a Cl^- conductance. Furthermore, we observed that the application of a CB_2R antagonist slightly increased the firing rate, indicative of a certain eCB tonus and/or a constitutive activity of the receptor. These results are in line with both the emerging idea that the eCB system consists of a basal and an "on demand" pool of endocannabinoids and with the possibility of constitutively active CB_2Rs (39–41).

The mode of action we report here could be the underlying mechanism involved in the reduction of firing activity by JWH-133 in wide-range dorsal horn neurons in a rat model of acute, inflammatory, and neuropathic pain (20) and in thalamic neurons in a rat model of neuropathic pain (42).

The unique aspects of eCB signaling we describe in this study, uncover a modulatory role for the eCB system in mPFC function, through the regulation of neuronal excitability by CB_2R activation. Because high frequency stimulation leads to eCB synthesis (43), activation of CB_2Rs after increased neuronal activity may prevent excessive neuronal firing via an intracellularly organized feedback system. Through this mechanism, CB_2Rs could play a protective role in the brain (44). More generally, the differential (sub)cellular localization of CB_1Rs and CB_2Rs and their downstream pathways diversify the response repertoire of the neuronal eCB system beyond the generally accepted modulation of neurotransmission processes.

Materials and Methods

Western Blotting. Experiments were approved by the animal welfare committee of the University of Amsterdam. mPFC, brainstem, spleen, and skeletal muscle of 14-d-old male Wistar rats (Harlan) were rapidly dissected out in ice-

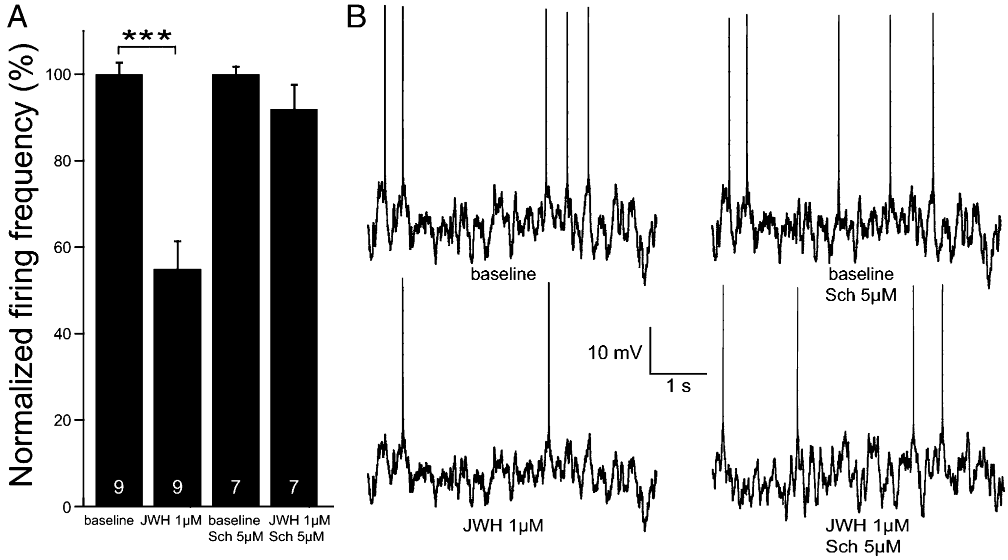

Fig. 4. CB_2R activation decreases firing activity of rat mPFC layer II/III pyramidal neurons. (*A*) Application of 1 μM JWH-133 led to a reduction of neuronal firing rate. Firing was induced by Gaussian current input into the soma. Mean baseline firing frequency of 0.88 ± 0.10 Hz was normalized over slices to 100 ± 3% and reduced to 55 ± 6% in the presence of 1 μM JWH-133 (****P* < 0.001). After preincubation (of at least 10 min before going whole-cell) with and continuous presence of 5 μM Sch.356036, baseline firing frequency 0.83 ± 0.15 Hz, normalized to 100 ± 3%, JWH-133 (1 μM) could not induce a response (92 ± 6%, JWH-133 plus Sch.356036). (*B*) Representative traces of current clamp recordings showing action potential firing of layer II/III neurons in the absence (baseline) and presence of 1 μM JWH-133 and in the presence of 5 μM Sch.356036 (Sch.356036 baseline) and 1 μM JWH-133 plus 5 μM Sch.356036.

cold homogenization buffer (0.05 mM PBS) with 320 mM sucrose and protease inhibitor mixture (Complete, pH 7.4; Roche) and homogenized with a glass douncer. For subcellular fractionation of the mPFC, the same buffer was used. The homogenate was centrifuged at 800 × g for 10 min to discard undisrupted tissue. The supernatant was centrifuged at 100,000 × g for 1 h to separate plasma membrane fractions (pellet) from intracellular fractions (supernatant). Equal amounts of protein, 10 or 20 μg, were loaded and separated by sodium dodecyl sulfate–polyacrylamide gel electrophoresis (SDS-PAGE) on 10% Tris-glycine gel and transferred onto nitrocellulose membrane. The membranes were washed in Tris-buffered saline (TBS) and blocked in TBS with 1% (vol/vol) Tween (TBST) containing 4% (wt/vol) nonfat milk and incubated overnight at 4 °C with antibodies against CB_2R (Abcam; 1:800) alone or in combination with antibodies against the plasma membrane marker Na^+/K^+-ATPase α3 (Santa Cruz Biotechnology; 1:500) and against the nuclear envelope marker nucleoporin p62 (Beckton Dickinson; 1:800). In some cases, the CB_2R antibody was preincubated with the immunogen peptide (Abcam; 1:40). Membranes were washed with TBST and incubated for 1 h with HRP-conjugated goat anti-rabbit antibody (Bio-Rad; 1:3,000), goat anti-mouse antibody (Bio-Rad, 1:3,000), and donkey anti-goat antibody (Santa Cruz Biotechnology; 1:5,000) and processed for immunoreactivities using enhanced chemiluminesence (ECL) Plus Western Blotting detection reagents (Amersham). Bands were visualized with Hyperfilm ECl (Amersham) or the Odyssey Infrared Imaging System (Licor).

Radioactive Binding Assay. CB_1R and CB_2R binding was assessed by rapid filtration assays, using 400 pM [^{3}H]CP55.940 as reported (45). mPFC tissue of 14-d-old male Wistar rats (Harlan) was used in rapid filtration assays, after subcellular fractionation as described for the Western blot samples in 2 mM Tris·EDTA, 320 mM sucrose, and 5 mM $MgCl_2$ at pH 7.4. Unspecific binding was determined in the presence of "cold" agonist (1 μM CP55.940) and was further corroborated by selective antagonists [0.1 μM SR141716 (SR1) for CB_1R or 0.1 μM SR144528 (SR2) for CB_2R]. Binding data were expressed as femtomole ligand bound per milligram of protein.

Electrophysiology. Coronal slices (300 μm) of the mPFC were obtained from male Wistar rats (Harlan) aged 14–19 d postnatal and male C57BL/6 Wt mice or male C57BL/6 CB_2R KO mice (The Jackson Laboratory) aged 14–19 d postnatal. Animals were killed by decapitation, and their brains rapidly were removed and placed in oxygenated (95% O_2–5% CO_2) ice cold (4 °C) adapted artificial cerebrospinal fluid (aaCSF: 120 mM choline chloride, 3.5 mM KCl, 0.5 mM $CaCl_2$, 6 mM $MgSO_4$, 1.25 mM NaH_2PO_4, 25 mM D-glucose, and 25 mM $NaHCO_3$). Slices were cut in aaCSF on a vibratome (VT1200S; Leica) and placed for 30 min in aCSF (120 mM NaCl, 3.5 mM KCl, 25 mM $NaHCO_3$, 25 mM D-glucose, 2.5 mM $CaCl_2$, 1.3 mM $MgSO_4$, and 1.25 mM NaH_2PO_4; $[Cl^-]_{out}$ = 128.5 mM) at 32 °C. Slices were kept at room temperature for at least 1 h before recording. Glass recording pipettes were pulled from borosilicate glass (Science Products) and had a resistance of 2–3 MΩ when filled with pipette solution (110 mM KGluconate, 30 mM KCl, 0.5 mM EGTA, 10 mM 4-(2-hydroxyethyl)-1-piperazineethanesulfonic acid (Hepes), 4 mM Mg-ATP, and 0.5 mM Na-GTP). For local application of JWH-133, a Picospritzer II device (General Valve) was used to deliver the compound to the recorded neurons with brief pressure pulses (500 ms). Modified aCSF with K^+-, Ca^{2+}-, and Na^+-channel blockers contained 70 mM NaCl, 3.5 mM KCl, 25 mM $NaHCO_3$, 25 mM D-glucose, 2.5 mM $CaCl_2$, 1.3 mM $MgSO_4$, 1.25 mM NaH_2PO_4, 25 mM TEACl, 5 mM 4-AP, 0.2 mM $CdCl_2$, and 0.0005 mM TTX; $[Cl^-]_{out}$ = 103.7 mM. Modified pipette solution with 30 mM $[Cl^-]_i$ contained 110 mM CH_3O_3SCs, 30 mM CsCl, 0.5 mM EGTA, 10 mM Hepes, 4 mM Mg-ATP, and 0.5 mM Na-GTP). Modified pipette solution with 4.95 mM $[Cl^-]_i$ contained: 135.05 mM CH_3O_3SCs, 4.95 mM CsCl, 0.5 mM EGTA, 10 mM Hepes, 4 mM Mg-ATP, and 0.5 mM Na-GTP. Introduction of CB_2R ligands into neurons was achieved by backfilling the recording pipettes. Whole-cell current and voltage clamp recordings were made at 32 °C from the soma of layer II/III pyramidal neurons. In the whole-cell current clamp configuration, we used a slow feedback system that guaranteed that current clamp recordings started at a membrane voltage of −80 mV (Figs. 1 and 3) or −70 mV (Fig. 4). In the whole-cell voltage clamp configuration with $[Cl^-]_i$ = 30 mM, currents were evoked, every 30 s until JWH-133–mediated currents were recorded, by a series of rectangular voltage steps (200-ms duration) from a holding potential of −80 mV to voltage potentials ranging from −90 to −20 mV in 10-mV increments. For experiments with $[Cl^-]_i$ = 4.95 mM, the currents were evoked from a holding potential of −50 mV. Input resistance was calculated from current responses to hyperpolarizing steps of −5 mV. Frozen filtered Gaussian noise (time constant = 10 ms) was injected via the patch pipette with a variance adjusted for each neuron to result in a mean spike frequency (≈0.85 Hz). The firing frequency was calculated by using 1-min bins. Before drug application (or at least 10 min after preincubation with Sch.356036), 5-min recordings were used as control. Drug effects were determined 3–15 min after application. Recordings were made by using an EPC9 patch-clamp amplifier controlled by PULSE software (HEKA Electronic) and in-house software running under Matlab (MathWorks). Signals were filtered at 2.9 kHz and sampled at 10 kHz. Series resistance ranged from 5 to 15 MΩ and was compensated to ≈65%. Signals were corrected for liquid junction potential. Current densities were calculated by using cell capacitance and expressed in pA/pF.

Data Analysis. Data were statistically tested with paired and unpaired Student's t tests unless otherwise stated. In the figures, the significance is indicated with asterisks (*$P < 0.05$, **$P < 0.01$, and ***$P < 0.001$).

Drugs. For the radioactive binding assay, the synthetic cannabinoid CP55.940 {5-(1,10-dimethyheptyl)-2-[1*R*,5*R*-hydroxy-2*R*-(3-hydroxypropyl)-cyclohexyl] phenol} was purchased from Sigma Chemical. [^{3}H]CP55.940 (126 Ci/mmol) was from PerkinElmer Life Sciences. SR141716 [*N*-piperidino-5-(4-chlorophenyl)-1-(2,4-dichlorophenyl)-4-methyl-3-pyrazole-carboxamide], and SR144528 {*N*-[(1S)-endo-1,3,3-trimethy-1-bicyclo[2.2.1]-heptan-2-yl]5-(4-choro-3-methyl-phenyl)-1-(4-methyl-benzyl)-pyrazole-3-carboxamide} were kind gifts from Sanofi-Aventis Recherche (Paris, France). For the electrophysiological experiments, JWH-133, HU-308, and Sch.356036 were generous gifts from Abbott Laboratories (Weesp, the Netherlands). Cannabinoid receptor ligands were dissolved in DMSO to 50 mM and diluted in aCSF that never contained a final concentration of DMSO higher than 0.1%. BAPTA, 2-APB, and DIDS were all purchased from Sigma-Aldrich. TTX (0.5 μM, Latoxan) was present during all recordings, with the exception of the experiments shown in Fig. 4.

ACKNOWLEDGMENTS. We thank Dr. N. L. M. Cappaert and Dr. J. A. van Hooft for critical reading of the manuscript and Dr. T. Z. Baram for critical suggestions in an early phase of the project. This study was supported by Dutch Top Institute Pharma Grant T5-107-1. M.B., S.O., and M.M. were supported by Fondazione TERCAS Grant 2009-2012 and by Fondazione Italiana Sclerosi Multipla Grant 2011-2012.

1. Pattij T, Wiskerke J, Schoffelmeer AN (2008) Cannabinoid modulation of executive functions. *Eur J Pharmacol* 585:458–463.
2. Bracey MH, Hanson MA, Masuda KR, Stevens RC, Cravatt BF (2002) Structural adaptations in a membrane enzyme that terminates endocannabinoid signaling. *Science* 298:1793–1796.
3. Devane WA, et al. (1992) Isolation and structure of a brain constituent that binds to the cannabinoid receptor. *Science* 258:1946–1949.
4. Dinh TP, et al. (2002) Brain monoglyceride lipase participating in endocannabinoid inactivation. *Proc Natl Acad Sci USA* 99:10819–10824.
5. Kano M, Ohno-Shosaku T, Hashimotodani Y, Uchigashima M, Watanabe M (2009) Endocannabinoid-mediated control of synaptic transmission. *Physiol Rev* 89:309–380.
6. Mechoulam R, et al. (1995) Identification of an endogenous 2-monoglyceride, present in canine gut, that binds to cannabinoid receptors. *Biochem Pharmacol* 50:83–90.
7. Herkenham M, et al. (1991) Characterization and localization of cannabinoid receptors in rat brain: A quantitative in vitro autoradiographic study. *J Neurosci* 11: 563–583.
8. Wilson RI, Nicoll RA (2001) Endogenous cannabinoids mediate retrograde signalling at hippocampal synapses. *Nature* 410:588–592.
9. Atwood BK, Mackie K (2010) CB2: A cannabinoid receptor with an identity crisis. *Br J Pharmacol* 160:467–479.
10. Galiegue S, et al. (1995) Expression of central and peripheral cannabinoid receptors in human immune tissues and leukocyte subpopulations. *Eur J Biochem* 232:54–61.
11. Munro S, Thomas KL, Abu-Shaar M (1993) Molecular characterization of a peripheral receptor for cannabinoids. *Nature* 365:61–65.
12. García-Gutiérrez MS, Pérez-Ortiz JM, Gutiérrez-Adán A, Manzanares J (2010) Depression-resistant endophenotype in mice overexpressing cannabinoid CB(2) receptors. *Br J Pharmacol* 160:1773–1784.
13. Gong JP, et al. (2006) Cannabinoid CB2 receptors: Immunohistochemical localization in rat brain. *Brain Res* 1071:10–23.
14. Liu QR, et al. (2009) Species differences in cannabinoid receptor 2 (CNR2 gene): Identification of novel human and rodent CB2 isoforms, differential tissue expression and regulation by cannabinoid receptor ligands. *Genes Brain Behav* 8:519–530.
15. Carlisle SJ, Marciano-Cabral F, Staab A, Ludwick C, Cabral GA (2002) Differential expression of the CB2 cannabinoid receptor by rodent macrophages and macrophage-like cells in relation to cell activation. *Int Immunopharmacol* 2:69–82.
16. Onaivi ES, et al. (2006) Discovery of the presence and functional expression of cannabinoid CB2 receptors in brain. *Ann N Y Acad Sci* 1074:514–536.
17. Stella N (2010) Cannabinoid and cannabinoid-like receptors in microglia, astrocytes, and astrocytomas. *Glia* 58:1017–1030.
18. Van Sickle MD, et al. (2005) Identification and functional characterization of brainstem cannabinoid CB2 receptors. *Science* 310:329–332.
19. Viscomi MT, et al. (2009) Selective CB2 receptor agonism protects central neurons from remote axotomy-induced apoptosis through the PI3K/Akt pathway. *J Neurosci* 29:4564–4570.
20. Elmes SJ, Jhaveri MD, Smart D, Kendall DA, Chapman V (2004) Cannabinoid CB2 receptor activation inhibits mechanically evoked responses of wide dynamic range dorsal horn neurons in naïve rats and in rat models of inflammatory and neuropathic pain. *Eur J Neurosci* 20:2311–2320.
21. Morgan NH, Stanford IM, Woodhall GL (2009) Functional CB2 type cannabinoid receptors at CNS synapses. *Neuropharmacology* 57:356–368.
22. Xi ZX, et al. (2011) Brain cannabinoid CB_2 receptors modulate cocaine's actions in mice. *Nat Neurosci* 14:1160–1166.
23. Zoratti C, Kipmen-Korgun D, Osibow K, Malli R, Graier WF (2003) Anandamide initiates Ca(2+) signaling via CB2 receptor linked to phospholipase C in calf pulmonary endothelial cells. *Br J Pharmacol* 140:1351–1362.
24. Frings S, Reuter D, Kleene SJ (2000) Neuronal Ca2+ -activated Cl- channels—homing in on an elusive channel species. *Prog Neurobiol* 60:247–289.
25. Brusco A, Tagliaferro P, Saez T, Onaivi ES (2008) Postsynaptic localization of CB2 cannabinoid receptors in the rat hippocampus. *Synapse* 62:944–949.
26. Brusco A, Tagliaferro PA, Saez T, Onaivi ES (2008) Ultrastructural localization of neuronal brain CB2 cannabinoid receptors. *Ann N Y Acad Sci* 1139:450–457.
27. Onaivi ES, et al. (2008) Functional expression of brain neuronal CB2 cannabinoid receptors are involved in the effects of drugs of abuse and in depression. *Ann N Y Acad Sci* 1139:434–449.
28. Onaivi ES, Ishiguro H, Gu S, Liu QR (2011) CNS effects of CB2 cannabinoid receptors: Beyond neuro-immuno-cannabinoid activity. *J Psychopharmacol* 10.1177/0269881111400652.
29. Ashton JC (2011) The use of knockout mice to test the specificity of antibodies for cannabinoid receptors. *Hippocampus* 10.1002/hipo.20946.
30. Jong YJ, Kumar V, Kingston AE, Romano C, O'Malley KL (2005) Functional metabotropic glutamate receptors on nuclei from brain and primary cultured striatal neurons. Role of transporters in delivering ligand. *J Biol Chem* 280:30469–30480.
31. Lee DK, et al. (2004) Agonist-independent nuclear localization of the Apelin, angiotensin AT1, and bradykinin B2 receptors. *J Biol Chem* 279:7901–7908.
32. Currie S, et al. (2008) IP(3)R-mediated Ca(2+) release is modulated by anandamide in isolated cardiac nuclei. *J Mol Cell Cardiol* 45:804–811.
33. Beltramo M (2009) Cannabinoid type 2 receptor as a target for chronic - pain. *Mini Rev Med Chem* 9:11–25.
34. Demuth DG, Molleman A (2006) Cannabinoid signalling. *Life Sci* 78:549–563.
35. Sagar DR, et al. (2005) Inhibitory effects of CB1 and CB2 receptor agonists on responses of DRG neurons and dorsal horn neurons in neuropathic rats. *Eur J Neurosci* 22:371–379.
36. Hartzell C, Putzier I, Arreola J (2005) Calcium-activated chloride channels. *Annu Rev Physiol* 67:719–758.
37. Andersen P, Dingledine R, Gjerstad L, Langmoen IA, Laursen AM (1980) Two different responses of hippocampal pyramidal cells to application of gamma-amino butyric acid. *J Physiol* 305:279–296.
38. Staley KJ, Mody I (1992) Shunting of excitatory input to dentate gyrus granule cells by a depolarizing GABAA receptor-mediated postsynaptic conductance. *J Neurophysiol* 68:197–212.
39. Alger BE, Kim J (2011) Supply and demand for endocannabinoids. *Trends Neurosci* 34: 304–315.
40. Atwood BK, Wager-Miller J, Haskins C, Straiker A, Mackie K (2012) Functional selectivity in CB2 cannabinoid receptor signaling and regulation: Implications for the therapeutic potential of CB2 ligands. *Mol Pharmacol* 81:250–263.
41. Di Marzo V (2011) Endocannabinoid signaling in the brain: Biosynthetic mechanisms in the limelight. *Nat Neurosci* 14:9–15.
42. Jhaveri MD, et al. (2008) Evidence for a novel functional role of cannabinoid CB(2) receptors in the thalamus of neuropathic rats. *Eur J Neurosci* 27:1722–1730.
43. Brown SP, Brenowitz SD, Regehr WG (2003) Brief presynaptic bursts evoke synapse-specific retrograde inhibition mediated by endogenous cannabinoids. *Nat Neurosci* 6: 1048–1057.
44. Pacher P, Mechoulam R (2011) Is lipid signaling through cannabinoid 2 receptors part of a protective system? *Prog Lipid Res* 50:193–211.
45. Maccarrone M, et al. (2008) Anandamide inhibits metabolism and physiological actions of 2-arachidonoylglycerol in the striatum. *Nat Neurosci* 11:152–159.